

## Multiple Mode Current Flowing Passive Piezoelectric Shunt Controller

S. Behrens   S. O. R. Moheimani   A. J. Fleming

*School of Electrical Engineering and Computer Science  
The University of Newcastle NSW 2308 Australia*

(Received January 2002)

A method for multiple mode piezoelectric shunt damping will be presented in this paper. The proposed “current flowing” shunt controller has a number of benefits compared to previous shunt damping schemes; it is simpler to implement and requires small number of passive circuit elements. The passive control strategy is validated through experimentation on two piezoelectric laminated structures.

©2002 Academic Press

### 1. INTRODUCTION

Placing an electrical impedance across the terminals of a piezoelectric transducer, which is normally bonded to or embedded in the host structure, is referred to as piezoelectric shunt damping. As the piezo-laminated structure strains, an electrical charge forms on the terminals of the transducer. By placing an appropriate passive electrical impedance across the terminals of the transducer, the circuit network is capable of increasing the mechanical damping.

Forward [1], experimentally demonstrated the use of resistive and inductive-resistive resonant piezoelectric shunt circuits. Hagood and von Flotow [2] later presented an analytical model for resistive and inductive-resistive shunt dampened systems. Other researchers, such as [3–5], have attempted to extend shunt damping to multiple modes. Currently, single and/or multiple mode shunts require large inductors to dampen low frequency modes. Consequently, active inductors are synthesized using operational amplifiers [6] and digital signal processor [7].

In this paper, we present a new passive multiple mode piezoelectric vibration dampener. The effect of the “current flowing” shunt controller is studied theoretically and then validated experimentally on two resonant structures. The current flowing shunt controller is similar in nature to “current blocking” circuits [5], as only a single piezoelectric transducer is used to control vibration of several modes. While achieving comparable performance to that of the current blocking shunt controller, the proposed controller has a number of advantages; it is simpler to implement as it requires a smaller number of components, requires no “floating” inductors [6], and the controller is inherently multiple mode and guaranteed to be stable.

The paper is organized as follows. Section 2 introduces a method for modeling a

piezoelectric transducer. Section 3 considers two piezoelectric laminated structures. Subspace system identification is employed to obtain a model for each system. In section 4, a method for modeling the piezoelectric composite system, i.e. the damped structure is developed. The next section, Section 5, presents the proposed “current flowing” shunt controller. Section 6, reports experimental results that verify the proposed control scheme. Finally in Section 7, the paper is concluded.

## 2. DYNAMIC MODELING FOR PIEZOELECTRIC SHUNT DAMPING

### 2.1. PIEZOELECTRIC MODEL

Piezoelectric crystals have the unique ability to convert mechanical strain into electrical energy and *vice versa*. For vibration control, a thin layer of piezoelectric material, normally lead titanate zirconate (PZT), is sandwiched between two conducting layers. This forms a piezoelectric transducer. The transducer is then glued to the surface of the flexible structure using a strong adhesive material.

A piezoelectric transducer behaves electrically like a capacitor  $C_p$  and mechanically like a stiff spring. It is common practice to model the piezoelectric element as a capacitor  $C_p$  in series with a strain dependent voltage source  $v_p$  [2, 8, 9], as shown in Figure 1. As discussed in [10, 11], for small mechanical strains, the piezoelectric strain-voltage relations is relatively linear.

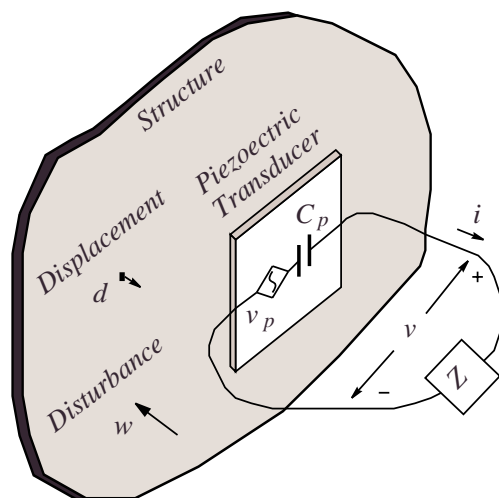


Figure 1. A piezoelectric shunted structure.

### 2.2. MODELING THE PIEZOELECTRIC SHUNT SYSTEM

Consider Figure 1, where a piezoelectric transducer is adhered to the surface of a linear elastic structure. As the structure deforms, due to a point disturbance  $w$ , an electric charge forms on the conducting plates of the piezoelectric transducer. Since a charge has formed on the terminals of the piezoelectric transducer, a current flows

through the impedance  $Z$ . Hence, mechanical energy is transformed to electrical energy which is subsequently dissipated by the resistive component of  $Z$ .

To make the discussion clearer, the shunt impedance  $Z$  is removed from the circuit, i.e., the piezoelectric transducer is open circuited, then the voltage across the terminals of the transducer is equivalent to  $v_p$ . The voltage  $v_p$  is entirely due to the disturbance  $w$  acting on the structure. Therefore,  $v_p$  is related to  $w$  via a transfer function  $G_{wv}$ . That is,

$$v_p(s) = G_{wv}(s)w(s), \quad Z(s) = \infty. \quad (1)$$

Alternatively, if we apply a voltage at  $v$  and measure the displacement at a point on the structure  $d$ , then the related transfer function between  $v$  to  $d$  is  $G_{vd}$ . Such that,

$$d(s) = G_{vd}(s)v(s), \quad Z(s) = \infty \quad w(s) = 0. \quad (2)$$

Note the conditions  $Z(s) = \infty$  and  $w(s) = 0$ , where the piezoelectric shunting layer terminals are open circuited and the point disturbance is set to zero, respectively.

Now, assume no disturbance is acting on the structure, i.e.,  $w(s) = 0$ , while a voltage source  $v(s)$  is attached to the terminals of the piezoelectric transducer. In this case, the transfer function from  $v_p$  to  $v$  is  $G_{vv}(s)$ . That is,

$$v_p(s) = G_{vv}(s)v(s), \quad w(s) = 0. \quad (3)$$

If the structure is disturbed by a voltage  $\hat{v}$  applied to an identical collocated piezoelectric transducer and some impedance  $Z$  is attached to the piezoelectric terminals, then the overall linear relationship is

$$v_p(s) = G_{vv}(s)\hat{v}(s) - G_{vv}(s)v(s). \quad (4)$$

Furthermore, Ohm's law states that the voltage  $v$  is related to current  $i$  via

$$v(s) = Z(s)i(s). \quad (5)$$

Using Kirchoff's voltage law for Figure 1, we can analyze the piezoelectric shunt circuit voltage  $v$  as

$$v(s) = v_p(s) - \frac{i}{C_p s}, \quad (6)$$

where  $C_p$  is the capacitance of the piezoelectric shunting layer. Using (5) and (6), we obtain

$$v(s) = \frac{C_p s Z(s)}{1 + C_p s Z(s)} v_p(s). \quad (7)$$

Combining (4) and (7) using simple algebra, we can find the shunt transfer function  $\hat{G}_{vv}(s)$ , as

$$\hat{G}_{vv}(s) = \frac{v_p(s)}{\hat{v}(s)} = \frac{G_{vv}(s)}{1 + G_{vv}(s)K(s)}, \quad (8)$$

where  $K$  is defined as

$$K(s) = \frac{C_p s Z(s)}{C_p s Z(s) + 1}. \quad (9)$$

Equation (8) can also be used to obtain the displacement at a given point on the flexible structure, that is, the shunt transfer function  $\hat{G}_{vd}(s)$ , as

$$\hat{G}_{vd}(s) = \frac{d(s)}{\hat{v}(s)} = \frac{G_{vd}(s)}{1 + G_{vv}(s)K(s)}. \quad (10)$$

From the above equations, the reader may note that piezoelectric shunt damping is in fact a negative feedback control problem where  $K$  is the controller. For a more in-depth description of the shunt feedback scheme the reader is referred to [8, 12].

### 3. DEVELOPING THE “CURRENT FLOWING” SHUNT CONTROLLER

The “current flowing” shunt is similar in nature to “current blocking” circuit [5]. Instead of preventing the current from flowing at a specific frequency  $\omega_i$  ( $i = 1, 2, 3, \dots, n$ ), we allow the current to flow. This is achieved by using a series capacitor-inductor circuit  $C_i - \hat{L}_i$ , shown in Figure 2. The series  $C_i - \hat{L}_i$  is tuned to the structural resonance frequency  $\omega_i$ . The series capacitor-inductor circuit,  $C_i - \hat{L}_i$ , appears to be a short circuit at  $\omega_i$  and approximately open circuit for all other frequencies. While the shunting branch  $\tilde{L}_i - C_p$  is also tuned to  $\omega_i$ . Therefore, each circuit branch,  $C_i - \hat{L}_i - \tilde{L}_i - R_i$ , is functional at its own frequency  $\omega_i$ , but is approximately open circuit at all other frequencies. Notice that some level of interaction between modes that are closely spaced is expected. However, for modes that are widely spaced, this interaction will be minimal.

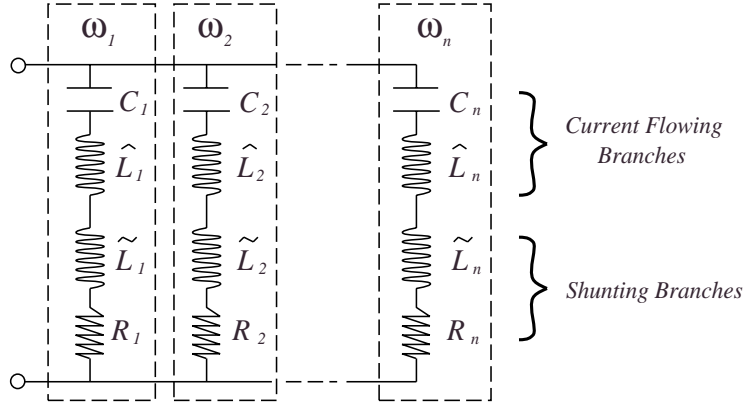


Figure 2. Proposed “current flowing” multiple mode shunt circuit.

#### 3.1. EXAMPLE “CURRENT FLOWING” SHUNT CONTROLLER FOR TWO MODES

To illustrate the proposed shunt circuit, consider the two mode case shown in Figure 3, at mode frequencies  $\omega_1$  and  $\omega_2$ . The first branch of the shunt circuit,

with shunt inductor  $\tilde{L}_1 = 1/(\omega_1^2 C_p)$  and  $R_1$ , is inserted with a “current flowing” circuit consisting of a series capacitor and inductor circuit  $C_1 - \hat{L}_1$  whose electrical impedance is designed to approach a short circuit at the branch frequency of  $\omega_1$  (as indicated with  $\omega_1$  in Figure 3). This is done by selecting  $C_1$  and  $\hat{L}_1$  such that the resonance frequency is at  $\omega_1 = 1/\sqrt{C_1 \hat{L}_1}$ , which is a fundamental characteristic of any resonant capacitor-inductor circuit. The “current flowing” circuit in the second branch also uses a resonant circuit whose electrical impedance approaches a short circuit at the second structural frequency of  $\omega_2$  by selecting  $C_2$  and  $\hat{L}_2$  such that  $\omega_2 = 1/\sqrt{C_2 \hat{L}_2}$ . When the two branches are connected together to the piezoelectric shunting layer terminals, each branch acts independently for their respective modes. That is, the first branch is designed to introduce damping at  $\omega_1$  while not disturbing the second branch that is approximately open circuit (i.e. the impedance is very large) at  $\omega_1$ . The same reason applies for the second branch.

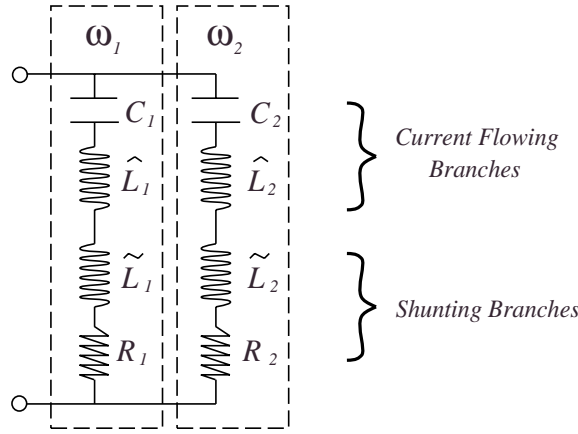


Figure 3. Proposed two mode “current flowing” shunt circuit.

### 3.2. GENERALIZED “CURRENT FLOWING” SHUNT CONTROLLER

For the generalized case, for  $n$  structural modes,

$$\tilde{L}_1 = \frac{1}{\omega_1^2 C_p}, \dots, \tilde{L}_n = \frac{1}{\omega_n^2 C_p} \quad (11)$$

where  $\tilde{L}_i$  is tuned into  $C_p$ . Frequencies  $\omega_i$  are the mode frequencies to be passively controlled and assuming that  $\omega_1 < \omega_2 < \dots < \omega_n$ . The relationship for  $\hat{L}_i$  current flowing branches is

$$\hat{L}_1 = \frac{1}{\omega_1^2 C_1}, \dots, \hat{L}_n = \frac{1}{\omega_n^2 C_n}. \quad (12)$$

By combining the series inductor values together (e.g.  $L_i = \tilde{L}_i + \hat{L}_i$ ),

$$L_1 = \frac{C_p + C_1}{\omega_1^2 C_1 C_p}, \dots, L_n = \tilde{L}_n + \hat{L}_n = \frac{C_p + C_n}{\omega_n^2 C_n C_p}, \quad (13)$$

the total impedance for each shunting branch  $Z_i(s)$  has been simplified. Therefore, the *modified* current flowing shunt, shown in Figure 4, has one less passive element in each shunting branch. The reader may note that the proposed *modified* controller, shown in Figure 4, resembles the circuit of Hollkamp [4]. However, there are significant differences between the two approaches.

One distinction is that the shunt circuit proposed in [4] includes only one resistor-inductor circuit for the first mode, while in our approach a resistor-inductor-capacitor circuit is used to shunt each mode. Furthermore, the methodology proposed here for determining the capacitive and inductive elements is very different to that suggested in [4]. The reader can observe that by following the above procedure, capacitors and inductors for each parallel branch of the circuit can be determined in a very straightforward manner. This is in contrast to the methodology proposed in [4], that requires the solution to a non-trivial optimization problem.

The total shunt branch impedance  $Z_i(s)$ , is

$$Z_1(s) = \frac{s^2 + \frac{R_1}{L_1}s + \frac{1}{L_1C_1}}{\frac{1}{L_1}s}, \quad \dots, \quad Z_n(s) = \frac{s^2 + \frac{R_n}{L_n}s + \frac{1}{L_nC_n}}{\frac{1}{L_n}s}, \quad (14)$$

or the admittance  $Y_i(s) = \frac{1}{Z_i(s)}$  is

$$Y_1(s) = \frac{\frac{1}{L_1}s}{s^2 + \frac{R_1}{L_1}s + \frac{1}{L_1C_1}}, \quad \dots, \quad Y_n(s) = \frac{\frac{1}{L_n}s}{s^2 + \frac{R_n}{L_n}s + \frac{1}{L_nC_n}}. \quad (15)$$

By summing the shunt branches together we derive the total shunt admittance, as

$$Y(s) = \sum_{i=1}^n Y_i(s) = \sum_{i=1}^n \frac{\frac{1}{L_i}s}{s^2 + \frac{R_i}{L_i}s + \frac{1}{L_iC_i}}. \quad (16)$$

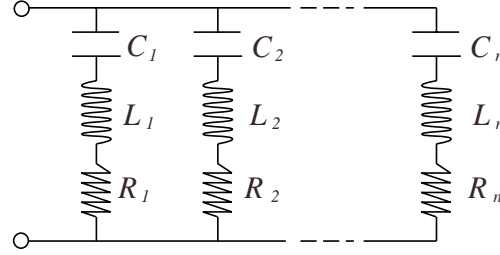


Figure 4. Proposed modified “current flowing” multiple mode shunt circuit.

Now, the feedback controller (9), can be determined as

$$K(s) = \frac{1}{1 + \frac{1}{C_p s} Y(s)}. \quad (17)$$

Using (16), it can be shown that the effective feedback controller is:

$$K(s) = \frac{1}{1 + \sum_{i=1}^n \frac{\frac{1}{L_i C_p}}{s^2 + \frac{R_i}{L_i}s + \frac{1}{L_i C_i}}} \quad (18)$$

or alternatively,

$$K(s) = \frac{\prod_{i=1}^n \left( s^2 + \frac{R_i}{L_i}s + \frac{1}{L_i C_i} \right)}{\prod_{i=1}^n \left( s^2 + \frac{R_i}{L_i}s + \frac{1}{L_i C_i} \right) + \sum_{i=1}^n \frac{1}{L_i C_p} \prod_{l=1, l \neq i}^n \left( s^2 + \frac{R_l}{L_l}s + \frac{1}{L_l C_l} \right)}. \quad (19)$$

Notice that the controller has a highly resonance structure. It applies a high gain at each target base structure resonant frequency. Viewing the shunted system in this manner has the advantage that the residual effects of each mode on other modes can be determined in a straightforward manner. It can be observed that as long as the controlled modes are reasonably spaced, this “residual effect” will be minimal. However, if two modes are very close, this effect can not be ignored and may degrade the performance of the shunted system at those specific resonance frequencies.

#### 4. PROPOSED “CURRENT FLOWING” SHUNT CONTROLLER VALIDATION

The proposed control scheme will be validated experimentally on two resonant structures; a simply supported beam, and a bounded plate structure. Photographs of the two piezoelectric laminate structures are shown in Figures 5 and 6. For both structures, two piezoelectric patches are bonded to the surface of each structure using a strong adhesive material. On each structure, one piezoelectric patch will be used as an actuator to generate a disturbance and the other as a shunting layer, as shown in Figure 7. For a detailed description of the apparatus, the reader is referred to [8, 12, 13].

In order to design an effective shunt controller it is necessary to obtain a model of the resonant system. Obtaining an analytic model for many realistic structure may not be possible since the flexible structure in question may be too difficult to model analytically. In such cases the technique of system identification may be helpful. Subspace based system identification techniques have proven to be an efficient means of identifying the dynamics of high order, highly resonant systems. A full summary of subspace based system identification techniques is described in reference [14].

When observing the dynamics of a structure, it is common practice to consider the transfer function between the displacement at some point on the structure and the disturbance actuator voltage applied to the actuating patch  $G_{vd}(s)$ . Another important transfer function is the dynamics between the shunting piezoelectric voltage (assuming  $Z(s) = \infty$ ) and the actuator voltage. Since the shunting layer voltage and actuating voltage are collocated, as shown in Figure 7, we can measure  $G_{vv}(s)$  directly.

For the two resonant structures we need to experimentally minimize the energy of the system. This can be achieved by minimizing the  $G_{vd}(s)$ , i.e. the disturbance

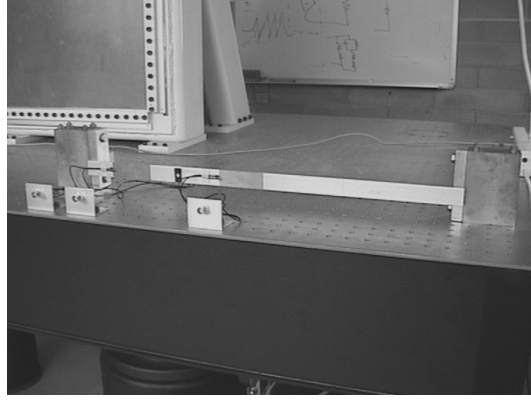


Figure 5. Piezoelectric laminated simply supported beam.

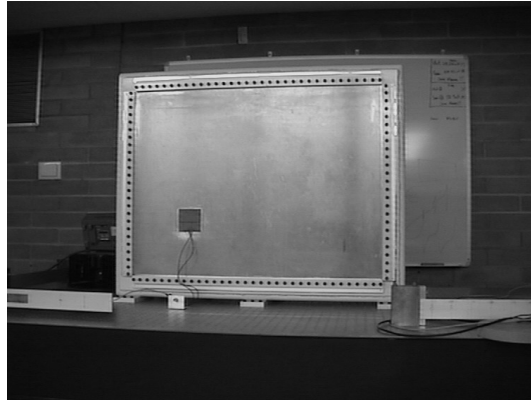


Figure 6. Piezoelectric laminated plate bounded structure.

actuator voltage to the displacement at a point on the structure, as this effectively minimizes the vibration.

Using a Polytec laser scanning vibrometer (PSV-300) and a Hewlett Packard spectrum analyzer (35670A), frequency responses were obtained for  $G_{vd}(s)$  and  $G_{vv}(s)$ . These are shown plotted in Figures 8 and 9 respectively. Using the subspace based system identification technique, a model was fitted to the experimental data, the measured and identified transfer functions are shown in Figures 8 and 9. In the bandwidth of interest, the identified models were found to be good representations of the piezoelectric laminated systems.

#### 4.1. SIMPLY SUPPORTED BEAM

From Figure 8, we can obtain the resonant modes of the laminated structure. The resonance frequencies for the structure are shown in Table 1. The  $2^{nd}$ ,  $3^{rd}$ ,  $4^{th}$  and  $5^{th}$  structural modes were chosen due to their highly resonant amplitudes.

Assuming the capacitance values  $C_2$ ,  $C_3$ ,  $C_4$  and  $C_5$  to be  $10nF$  and the experimentally measured piezoelectric shunt capacitance  $C_p$  is  $105.77nF$ , we can calculate



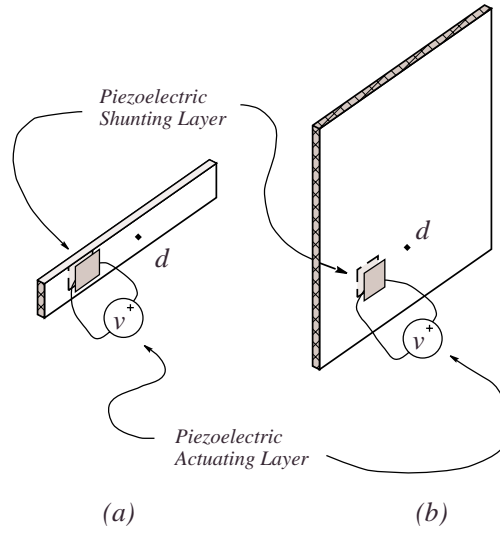


Figure 7. Experimental piezoelectric laminated structures: (a) simply supported beam and (b) plate bounded structure. Note  $v$  is the applied disturbance actuator voltage and  $d$  is the displacement at some point on the structure.

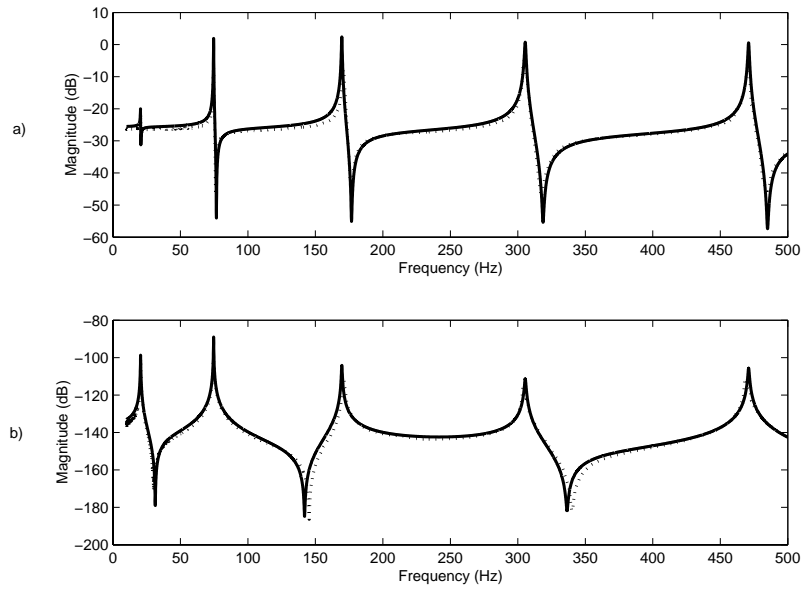


Figure 8. Frequency response a)  $|G_{vv}(s)|$  and b)  $|G_{vd}(s)|$ , for the piezoelectric laminated simply supported beam structure. Experimental data ( $\cdots$ ) and model obtained using subspace based system identification ( $—$ ).

the required inductance values using equation (13), as shown in Table 2.

In order to find the appropriate shunt resistance  $R_i$ , an optimization approach could be used. An optimization technique was proposed in [15], where the  $\mathcal{H}_2$  norm

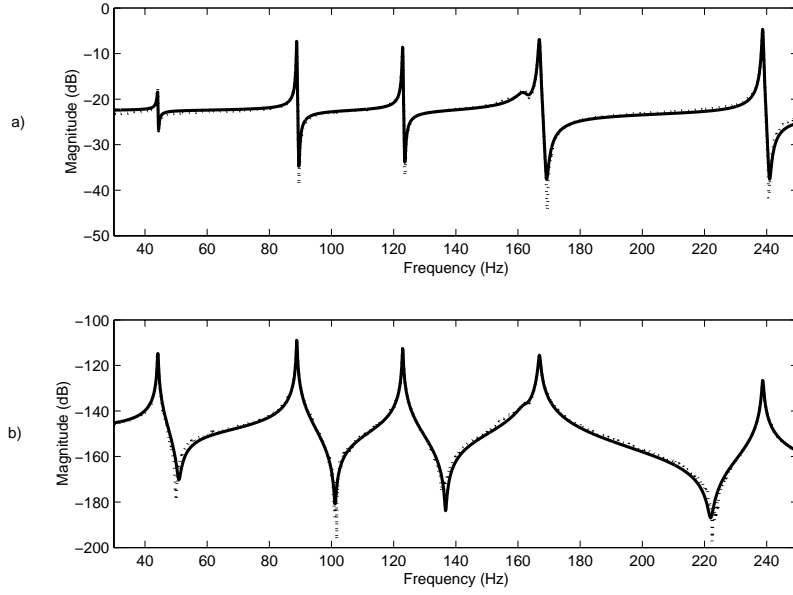


Figure 9. Frequency response a)  $|G_{vv}(s)|$  and b)  $|G_{vd}(s)|$ , for the piezoelectric laminated plate bounded structure. Experimental data ( $\cdots$ ) and model obtained using subspace based system identification ( $—$ ).

TABLE 1

*Experimental resonant frequencies for the simply supported beam.*

| Mode       | Value (Hz) |
|------------|------------|
| $\omega_2$ | 76         |
| $\omega_3$ | 173        |
| $\omega_4$ | 306        |
| $\omega_5$ | 472        |

of the controlled system is minimized. Optimal shunt resistance values obtained using this technique are displayed in Table 2.

Simulated results for  $|G_{vd}(s)|$  and  $|\hat{G}_{vd}(s)|$  the shunted transfer function from the disturbance voltage to displacement, show that the resonance amplitudes have been considerably dampened, as shown in Figure 10. Table 3 summarizes the simulated amplitude reductions for the 2<sup>nd</sup>, 3<sup>rd</sup>, 4<sup>th</sup> and 5<sup>th</sup> modes.

Using a synthetic impedance<sup>1</sup> [7] with the required current flowing shunt circuitry, the frequency response of the shunted structure can be measured using the laser scanning vibrometer. Figure 11 shows the experimentally measured displace-

<sup>1</sup> The term “synthetic impedance” denotes a two terminal device that has an arbitrary relationship between voltage and current at its terminals, assuming that the admittance is stable and proper [7].

TABLE 2  
*Circuit parameters for the simply supported beam.*

| Circuit Element | Value  |
|-----------------|--------|
| $L_2$           | 480.0H |
| $L_3$           | 92.6H  |
| $L_4$           | 29.6H  |
| $L_5$           | 12.4H  |
| $R_2$           | 1423Ω  |
| $R_3$           | 1212Ω  |
| $R_4$           | 913Ω   |
| $R_5$           | 798Ω   |

ment responses for  $|G_{vd}(s)|$  and  $|\hat{G}_{vd}(s)|$ . The experimental resonant amplitudes were successfully reduced, as summarized in Table 3.

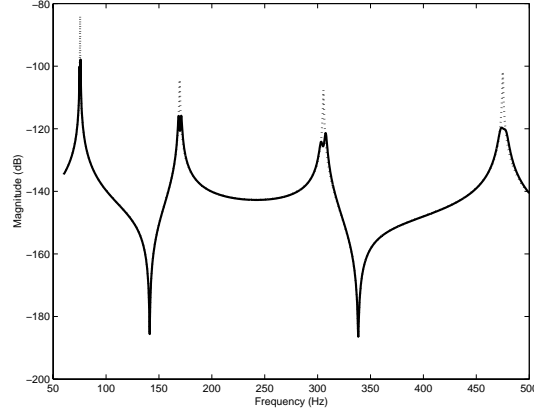


Figure 10. Simulated beam frequency response:  $|G_{vd}(s)|$  undamped response ( $\cdots$ ) and  $|\hat{G}_{vd}(s)|$  damped response ( $—$ ).

#### 4.2. PLATE BOUNDED STRUCTURE

Considering Figure 9, we can obtain the resonance frequencies of the bounded structure, they are shown in Table 4. The 1<sup>st</sup>, 2<sup>nd</sup>, 3<sup>rd</sup>, 5<sup>th</sup> and 6<sup>th</sup> structural modes were chosen due to their high resonant amplitudes. The 4<sup>th</sup> mode was neglected due to the reduced control authority and its proximity to the 5<sup>th</sup> mode.

Setting  $C_1, C_2, C_3, C_5$  and  $C_6$  to be  $7nF$ , and  $C_p$  equal to  $67.9nF$ , we can calculate the required inductance values, as shown in Table 5. The already mentioned  $\mathcal{H}_2$  norm optimization strategy is employed to determine the required resistance values, which are tabulated in Table 5.

TABLE 3

*Amplitude reduction for the simply supported beam.*

| Mode | Simulated (dB) | Experimental (dB) |
|------|----------------|-------------------|
| 2    | 14.5           | 13.5              |
| 3    | 8.2            | 7.8               |
| 4    | 14.1           | 13.8              |
| 5    | 16.4           | 15.8              |

TABLE 4

*Experimental resonant frequencies for the plate bounded structure.*

| Mode       | Value (Hz) |
|------------|------------|
| $\omega_1$ | 44.85      |
| $\omega_2$ | 90.2       |
| $\omega_3$ | 124.2      |
| $\omega_4$ | 161.6      |
| $\omega_5$ | 167.6      |
| $\omega_6$ | 237.2      |

TABLE 5

*Circuit parameters for the plate bounded structure.*

| Circuit Element | Value           |
|-----------------|-----------------|
| $L_1$           | 1986.3H         |
| $L_2$           | 491.1H          |
| $L_3$           | 259.2H          |
| $L_5$           | 142.2H          |
| $L_6$           | 71.1H           |
| $R_1$           | 2498.2 $\Omega$ |
| $R_2$           | 1858.3 $\Omega$ |
| $R_3$           | 1272.6 $\Omega$ |
| $R_5$           | 1641.5 $\Omega$ |
| $R_6$           | 1400.1 $\Omega$ |

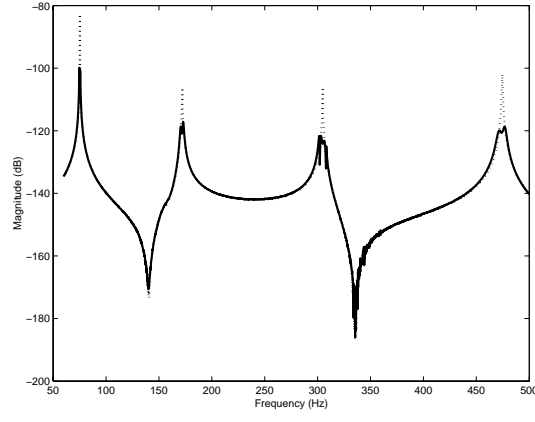


Figure 11. Experimental beam frequency response:  $|G_{vd}(s)|$  undamped response ( $\cdots$ ) and  $|\hat{G}_{vd}(s)|$  damped response ( $—$ ).

Simulated results for  $|G_{vd}(s)|$  and  $|\hat{G}_{vd}(s)|$  show that the structural amplitudes of the resonant structure have been dampened, as shown in Figure 12 and Table 6.

Using the synthetic impedance [7] and the laser scanning vibrometer, we can measure  $|G_{vd}(s)|$  and  $|\hat{G}_{vd}(s)|$ . The frequency response for the experimental undamped and damped systems are shown in Figure 13. Experimental results, shown in Figure 13, demonstrate that the structural modes of the bounded structure have been considerably damped. The experimental resonant amplitudes were successfully reduced, as shown in Table 6.

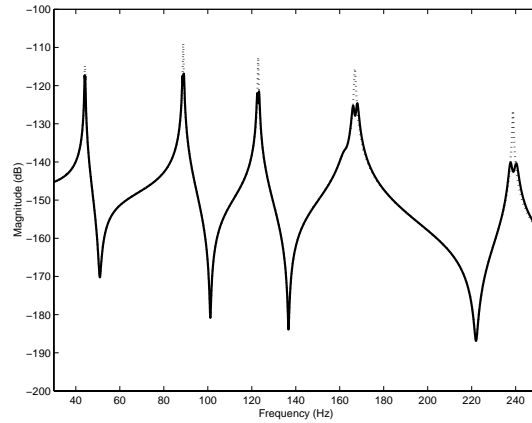


Figure 12. Simulated plate frequency response:  $|G_{vd}(s)|$  undamped response ( $\cdots$ ) and  $|\hat{G}_{vd}(s)|$  damped response ( $—$ ).

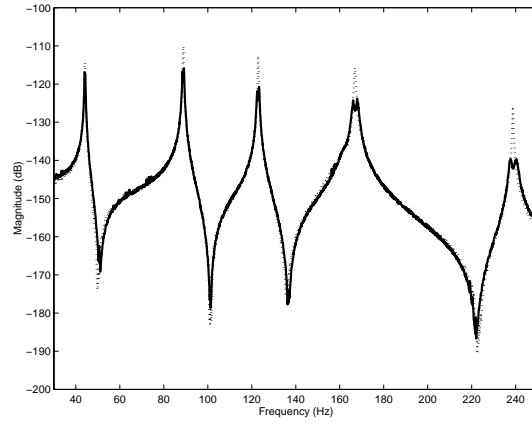


Figure 13. Experimental plate frequency response:  $|G_{vd}(s)|$  undamped response ( $\cdots$ ) and  $|\hat{G}_{vd}(s)|$  damped response ( $—$ ).

TABLE 6

*Amplitude reduction for the plate bounded structure.*

| Mode | Simulated (dB) | Experimental (dB) |
|------|----------------|-------------------|
| 1    | 3.2            | 3.8               |
| 2    | 10.9           | 10.1              |
| 3    | 13.2           | 12.8              |
| 5    | 13.9           | 13.2              |
| 6    | 15.8           | 14.7              |

## 5. CONCLUSION

The current flowing controller has been introduced as an alternative method for reducing structural vibrations. While achieving comparable performance to other passive control schemes, the current flowing piezoelectric shunt circuit has a number of advantages; it is simple - requires less resistors, capacitors and inductors; requires no “floating” inductors [6]; mode dominant - capable of damping more dominate resonant modes or neglecting the less dominant modes; multiple mode - can damp multiple modes using a single piezoelectric transducer; and passive - it is dissipative and guaranteed to be stable.

## ACKNOWLEDGEMENTS

This research was supported by the Centre for Integrated Dynamics and Control (CIDAC) and the Australian Research Council (ARC).

## REFERENCES

1. R. L. Forward, 1979 *Applied Optics* **18**, 690–697. Electronic damping of vibrations in optical structures.
2. N. W. Hagood and A. v. Flotow, 1991 *Journal of Sound and Vibration* **146**(2), 243–268. Damping of structural vibrations with piezoelectric materials and passive electrical networks.
3. D. L. Edberg, A. S. Bicos, C. M. Fuller, J. J. Tracy, and J. S. Fechter 1992 *Journal of Intelligent Materials Systems and Structures* **3**, 333–347. Theoretical and experimental studies of a truss incorporating active members.
4. J. J. Hollkamp 1994 *Journal of Intelligent Materials Systems and Structures* **5**, 49–56. Multimodal passive vibration suppression with piezoelectric materials and resonant shunts.
5. S. Y. Wu 1998 *Proceedings of the SPIE Smart Structures and Materials, Smart Structures and Intelligent Systems, SPIE Vol.3327*, 159–168. Method for multiple mode shunt damping of structural vibration using a single PZT transducer.
6. R. H. S. Riodan 1967 *Electronics Letters* **3**(2), 50–51. Simulated inductors using differential amplifiers.
7. A. J. Fleming, S. Behrens, and S. O. R. Moheimani 2000 *Electronics Letters* **36**(18), 1525–1526. Synthetic impedance for implementation of piezoelectric shunt damping circuits.
8. S. Behrens, 2001 Master’s thesis, University of Newcastle, Australia. Passive and semi-active vibration control of piezoelectric laminates.
9. J. J. Dosch, D. J. Inman, and E. Garcia 1992 *Journal of Intelligent Material Systems and Structures* **3**, 166–185. A self-sensing piezoelectric actuator for collocated control.
10. C. R. Fuller, S. J. Elliott, and P. A. Nelson 1996 Academic Press. *Active Control of Vibration*.
11. B. Jaffe, W. R. Cook, and H. Jaffe 1971 Academic Press. *Piezoelectric Ceramics*.
12. S. Behrens, A. J. Fleming, and S. O. R. Moheimani 2001 *Proceedings in SPIE Smart Structures and Materials, Damping and Isolation, SPIE Vol.4331*, 239–250. New method for multiple-mode shunt damping of structural vibration using a single piezoelectric transducer.
13. D. Halim and S. Moheimani 2001 To appear in *Journal of Mechatronics*. An optimization approach to optimal placement of collocated piezoelectric actuators and sensors on a thin plate.
14. T. McKelvey, A. J. Fleming, and S. O. R. Moheimani 2002 ASME *Journal of Vibration and Acoustics*, **124**(3), 429–464. Subspace based system identification for an acoustic enclosure.
15. S. Behrens and S. O. R. Moheimani 2001 Proceedings in IEEE *Conference on Decision and Control*, 4018–4023. Optimal resistive elements for multiple mode shunt-damping of a piezoelectric laminate beam.